Synoptic Aspects of Predictability of the Wintertime Arctic Oscillation

Vladimir Kryjov, Young-Mi Min

APEC Climate Center
Busan, Republic of Korea

Introduction

Introduction

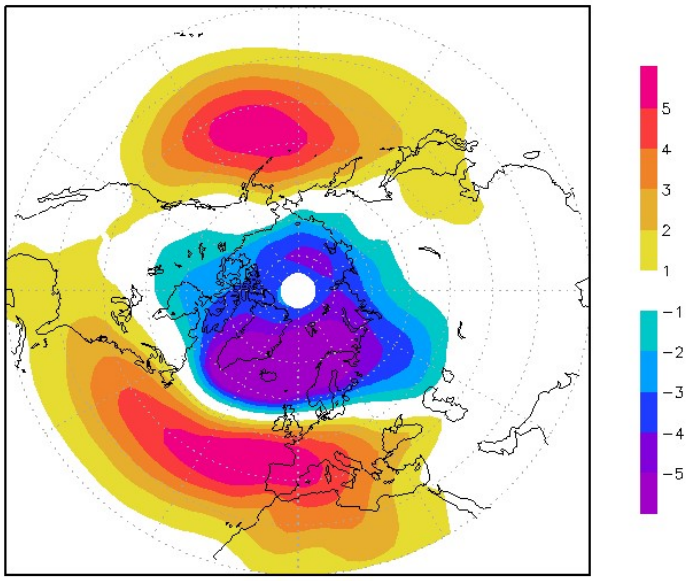

EOF1 (19%) of the mean monthly Z1000 anomalies (1979-2000).

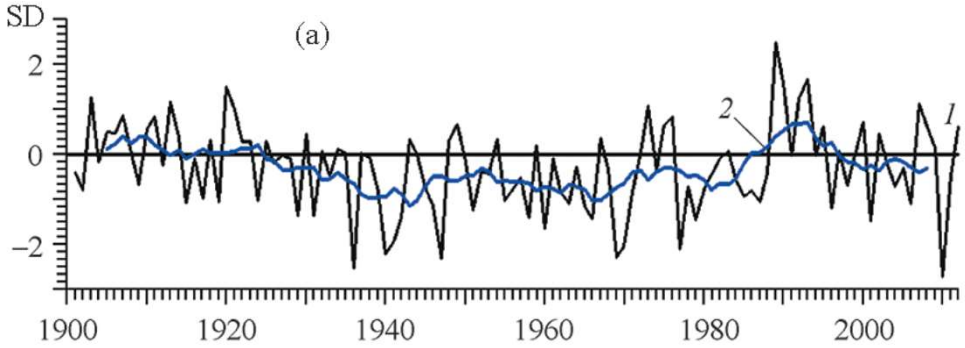

Time series of the normalized wintertime (December–March) AO index (*1*), and its 9-year running mean (*2*)

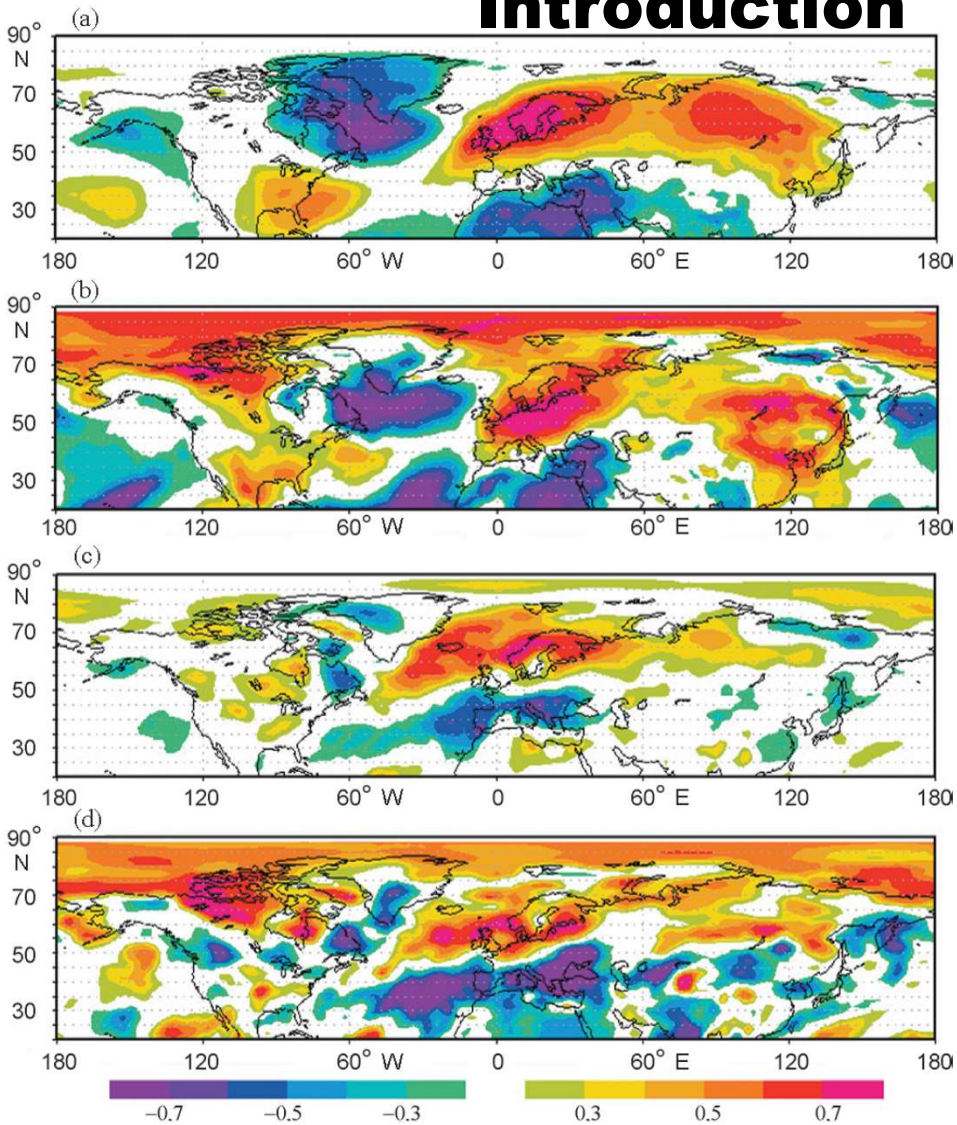

Correlations between the high frequency (a, c) and low frequency (b, d) components of the mean wintertime (December–March) values of (a, b) air temperature, (c, d) total precipitation, and the AO index (1905–2008).

Introduction

Current level of predictability of the wintertime AOI
(operational seasonal climate prediction models, one month lead)

•**Most common:** correlation < **0.2** on 20 - 30-year series.

•**Highest:**

-GloSea5 (14-year series): correlation **0.63**
(Scaife et al., 2014, MacLachlan et al., 2014).

- PNU (30-year series): correlation **0.60**
(Ahn and Kim, 2013; Sun and Ahn, 2014).

- CMCC (30-year series): correlation **0.55**
(Athanasiadis et al.,2014; Materia, 2016 (talk at APCC)).

That is, seasonal predictions of the most successful state-of-the-art models explain up to 30-40% of the variance of the wintertime AOI.

Introduction

Mechanism of the lag AO response to autumn influence beyond empirical studies

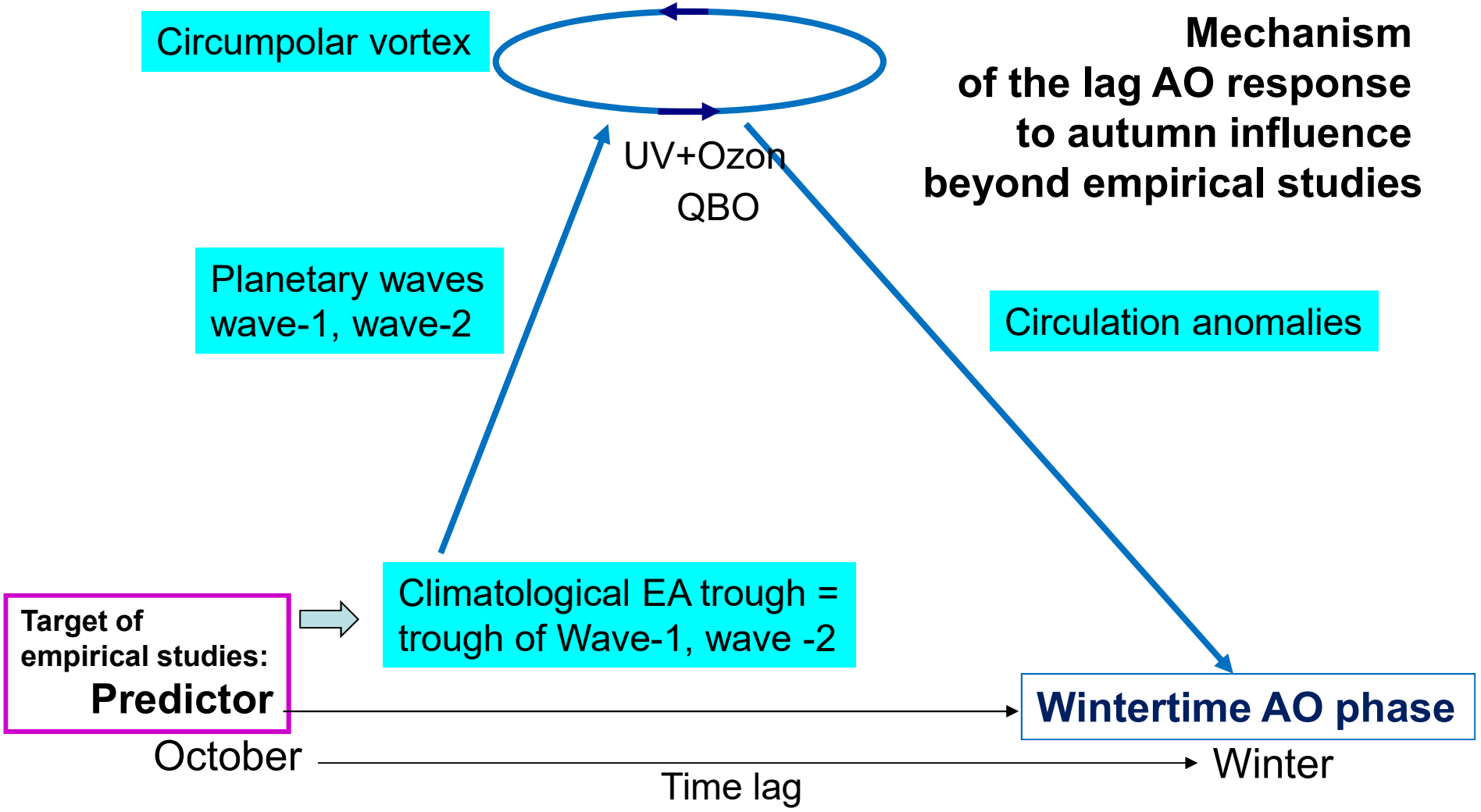

Mechanism description:

Theoretical: Charney and Drazin, 1961; Haynes et al., 1991; and others

Modelling: Shindel et al., 2001; Fletcher and Kushner, 2011, and others

Empirical: Baldwin and Dunkerton, 1999; Limpasuvan et al., 2005; Cohen et al., 2010, and others

Introduction

Mechanism of the lag AO response to autumn influence

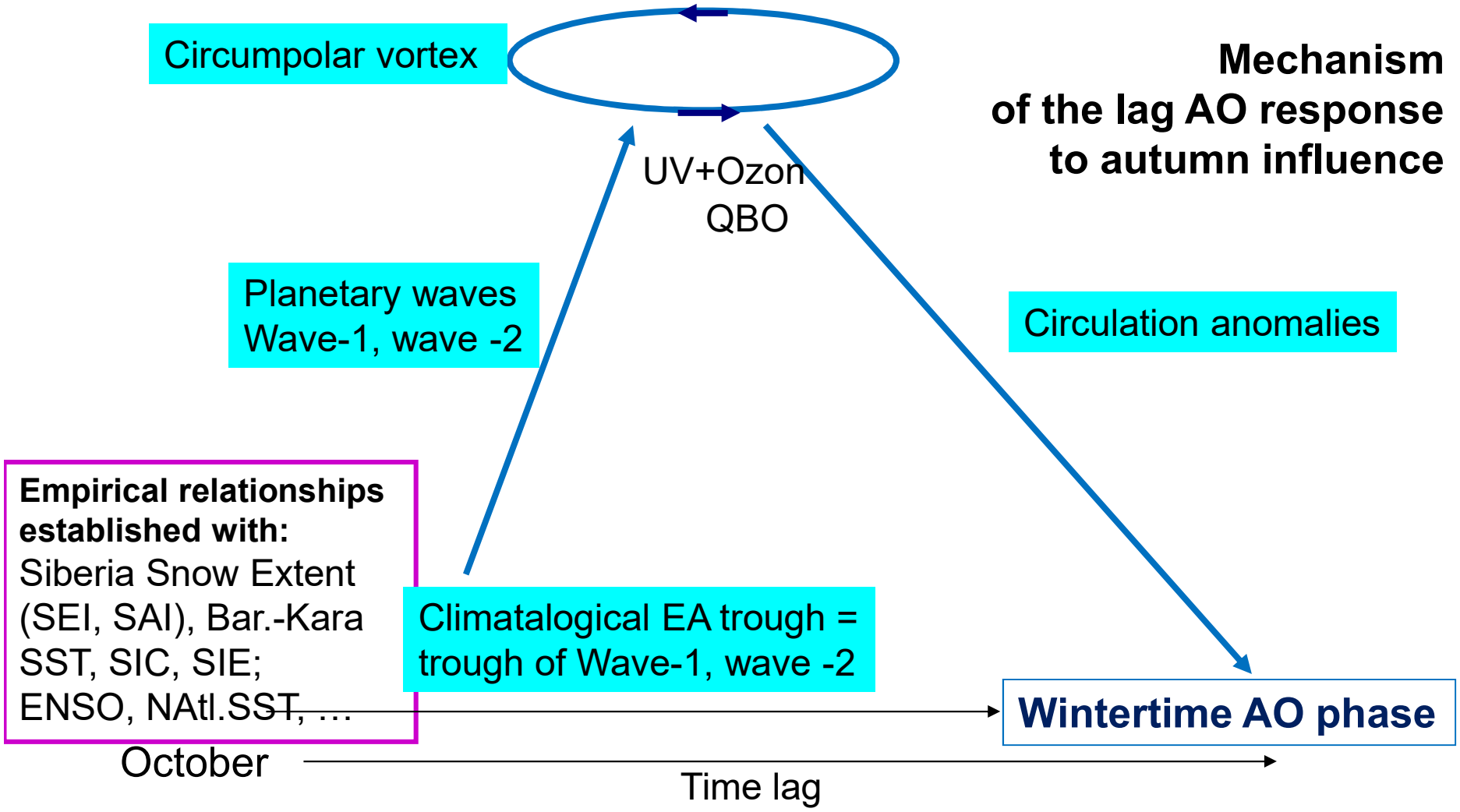

Empirical relationships:

Cohen et al., 2007; Cohen and Jones, 2011; Garfinkel et al., 2010; Deser et al. 2010; Liu et al. 2012; Folland et al., 2012; Scaife et al., 2014, Hall et al., 2015; Kryjov, 2015; and others

Introduction

October **TCI** (Z700 anomaly over the Taymyr Peninsula) yields a correlation of **0.58** with the DJF AO index on **dependent** 55-year series (Kryjov, 2015)

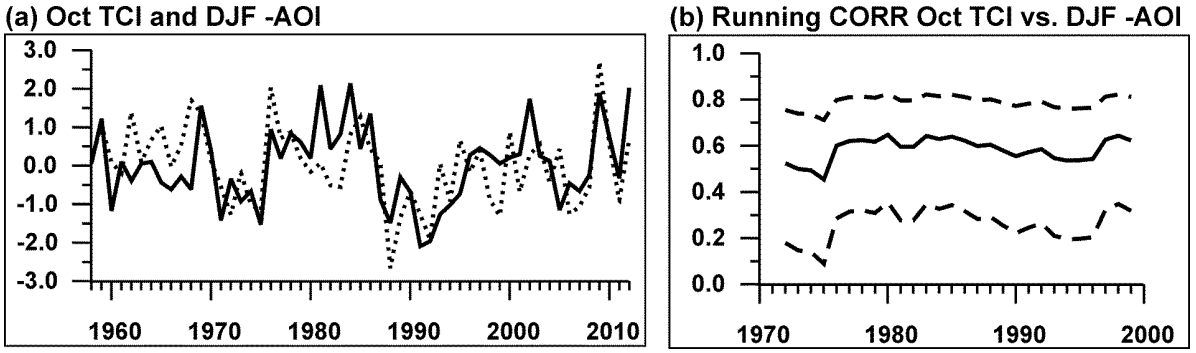

(a) Time series of October TCI (solid line) and inverted DJF AOI (dots), with both series normalized with respect to a 1958 - 2012 base period. R=0.58
(b) Running correlations calculated over 27 yr. windows (plotted in central year of 27 yr. periods) between October TCI and inverted DJF AOI (solid) and their 95% confidence intervals (dashed)

In the next study (Kryjov & Min, 2016) **this relationship is tested in a prediction mode on (quasi-)independent data and yeilds quite optimistic results.**

This presentation shows results from these studies focusing on the synoptic processes underlying predictability of the wintertime AO.

Data and Method of Prediction

Data

Reanalysis I: SLP, ZXXXs,

Reanalysis II: T2m

20CR: Precipitation, Snow cover

HISST: SST, SIC

55 winters: 1958/59 – 2012/13

Time structure of the performed experiment

Simulation of real-time forecast procedures

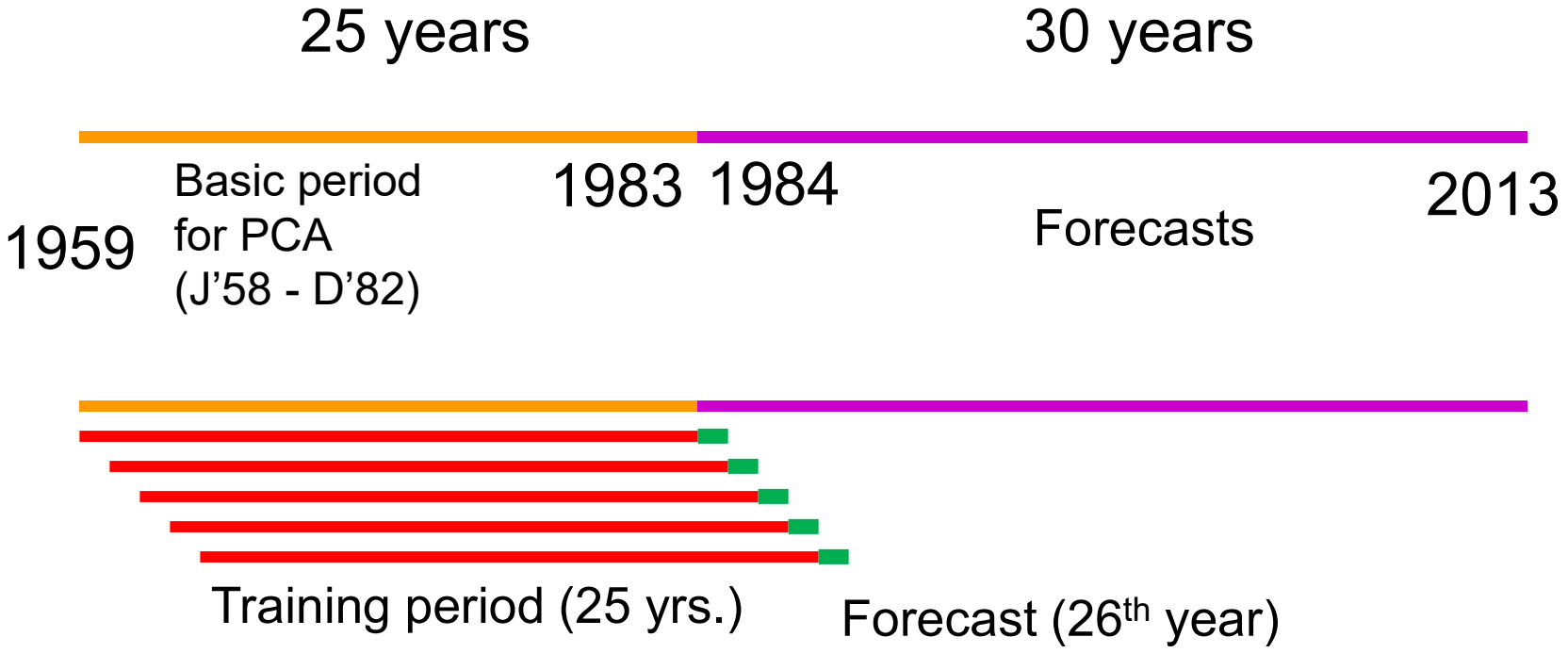

Total: 30 forecasts with a 1 year increment

Year as of January (e.g., the 1959 mark corresponds to D'58 – F'59)

Method of each year forecast

1. Oct. Z500 N of 20N 25 yrs. × 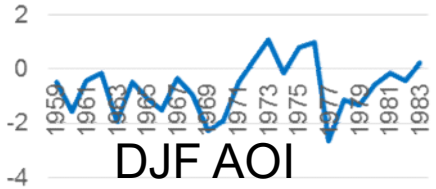

DJF AOI 25 yrs. → Corr. Map N of 20N

2. Oct. Z500 25 yrs. × Corr. map → 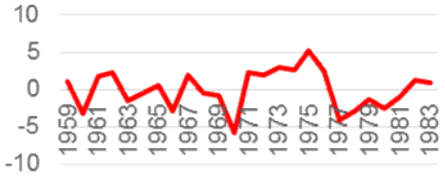

Predictor 25 yrs.

No restrictions on corr. value

3. 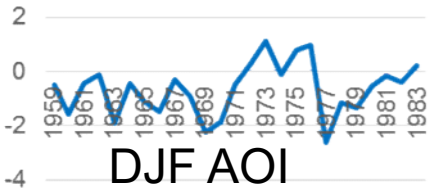

DJF AOI × 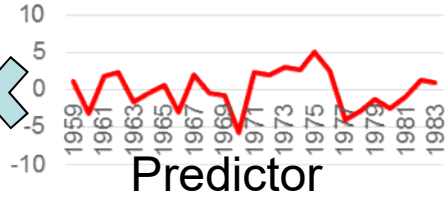

Predictor → DJF_AOI = a + b * Predictor

4. Oct. Z500 26th yr. × Corr. map → Predictor(yr.=26)

5. **Forecast: DJF_AOI(yr.=26) = a + b * Predictor(yr.=26)**

Prediction resulta

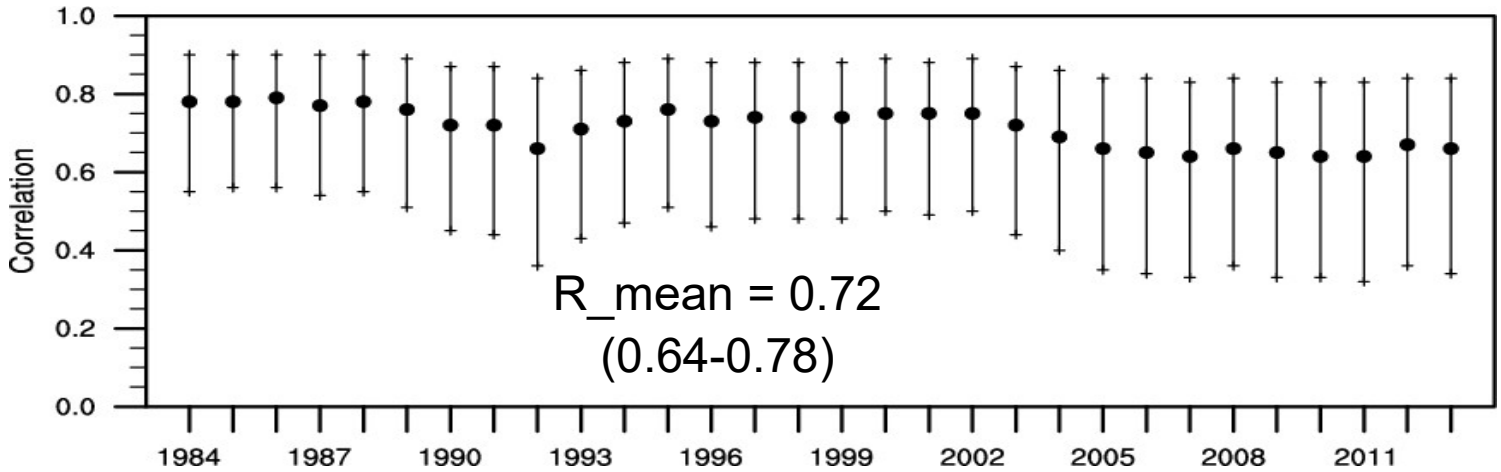

Predictors: Correlations between the constructed predictors and the wintertime AOI for the sliding 25-year training periods plotted at the forecast years

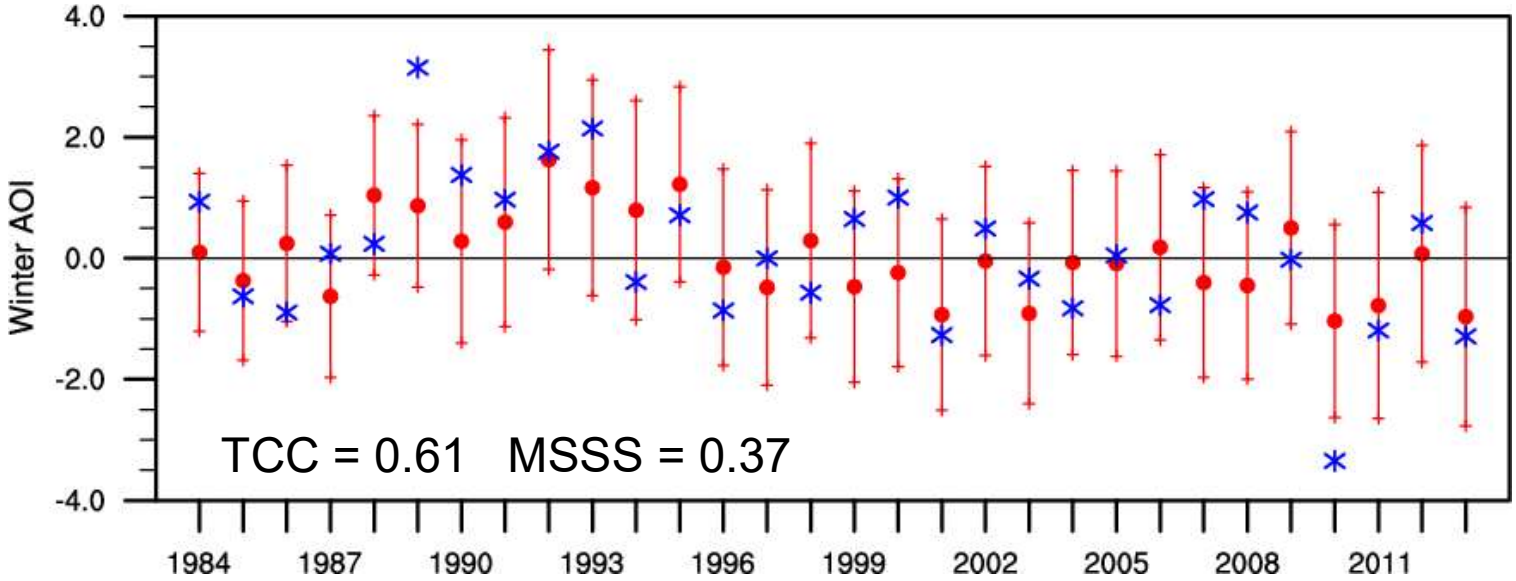

Result: DJF AOI: Observations (blue), Forecasts (red)

(Kryjov & Min, 2016)

What is beyond?

Summary of the correlation maps

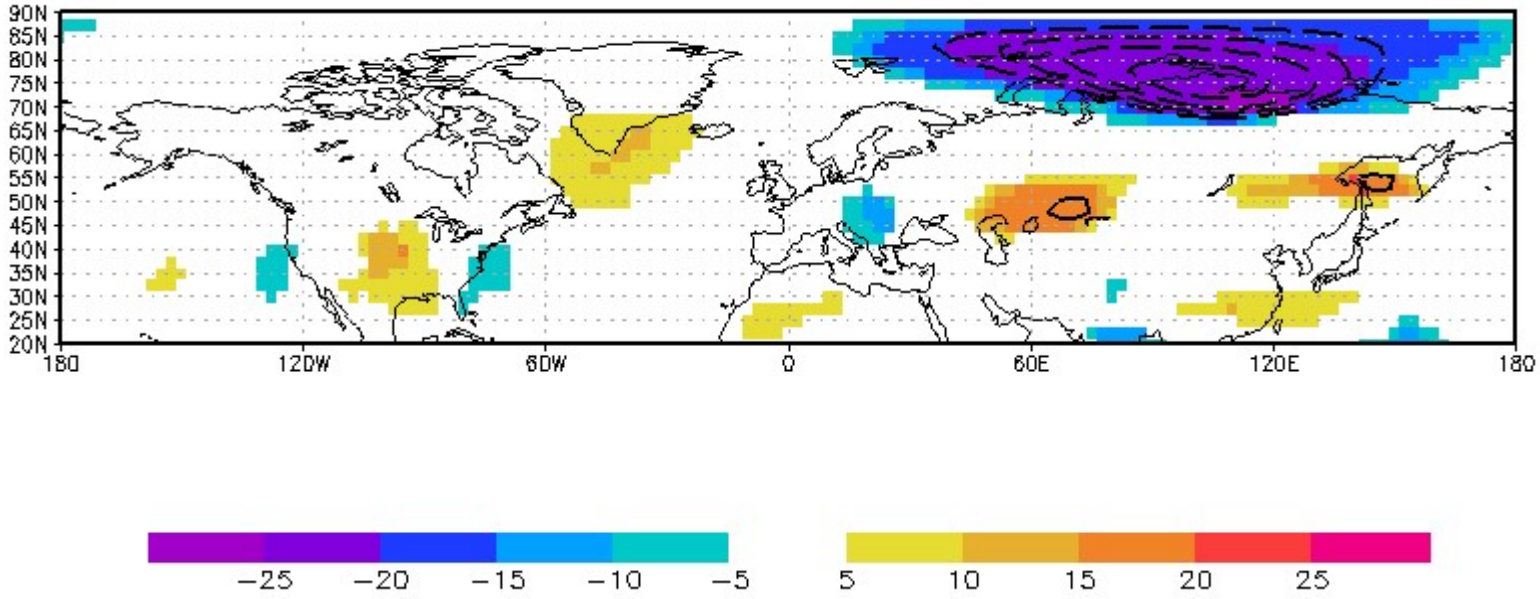

Shading: The number of forecasts (out of 30) with absolute value of correlation coefficients between the DJF AO and gridpoint series of Z500 during the training period being above 0.4. The sign corresponds to the sign of 30-yr average correlation.

Contours: mean correlation coefficients between the DJF AO and constructed predictors (correlations underlying regression). Values between -0.3 and +0.3 are omitted.

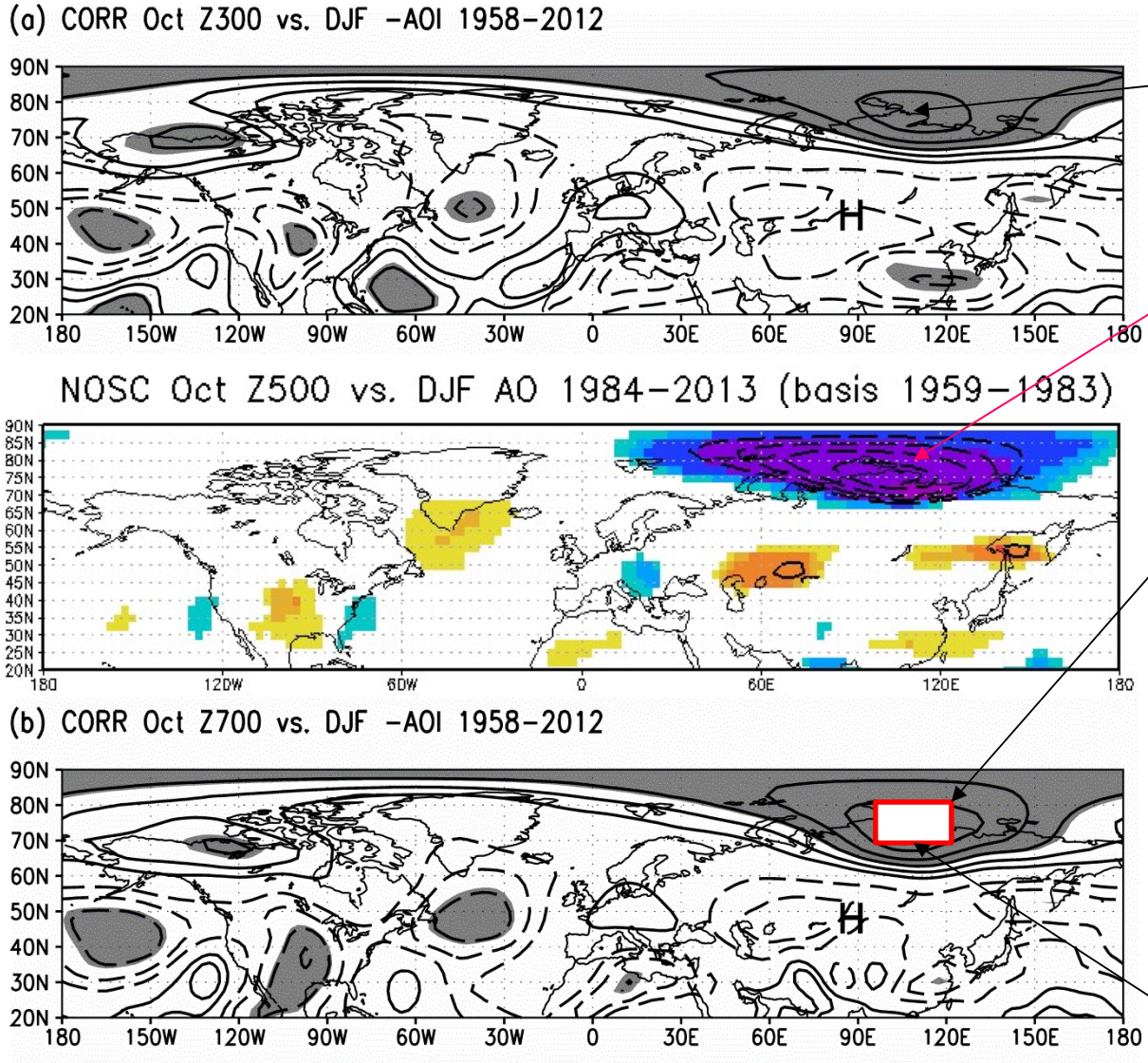

TCA

Correlations between October Z300 (a), Z700 (b), SLP (c) and the inverted DJF AOI for 1958 - 2012.

Contour interval is 0.1, negative values are dashed, the 0 value is omitted. The area where the correlations are significant at the 5% level in a two-tailed test is shaded

Definition of TCI
(80-70N, 100-120E)

B&W figures from Kryjov (2015)

Particular TCA mechanisms

Illustration corresponds to Oct TCA+ and DJF AO-

Positive tropospheric temperature anomaly

Climatological East Asia Trough (wave-1 & wave-2)

Negative tropospheric temperature anomaly

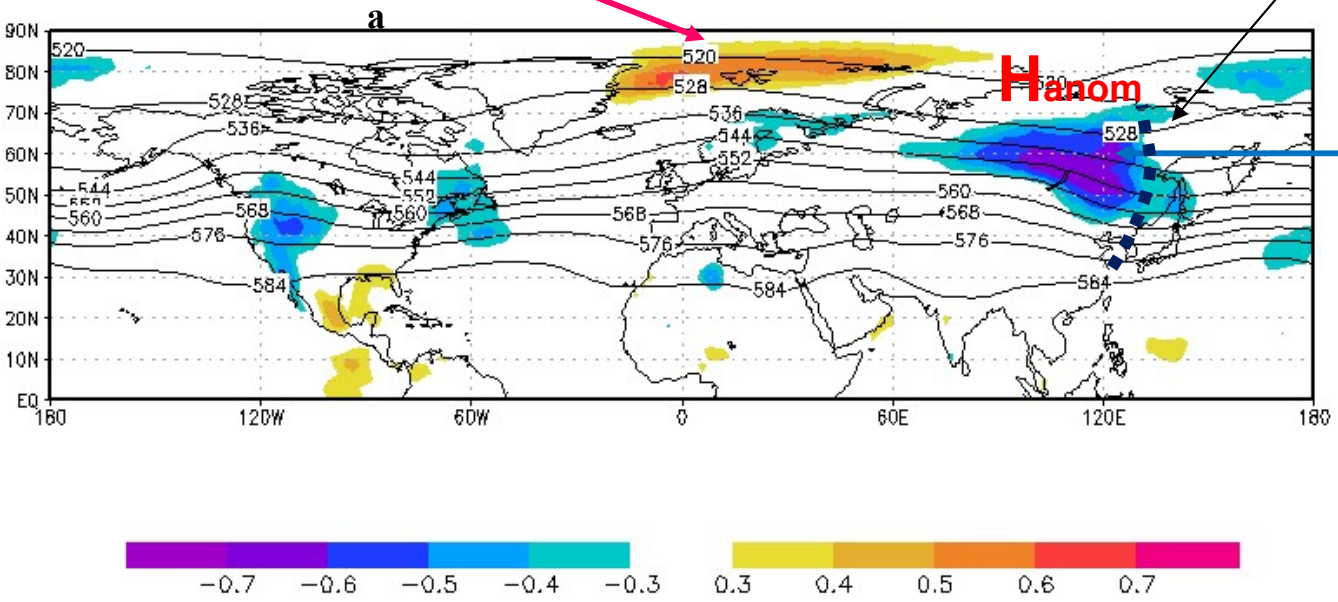

Correlations between October T2m and TCI. (1979-2010). Contours – Z500 climatology.

Illustration corresponds to Oct TCA+ and DJF AO-

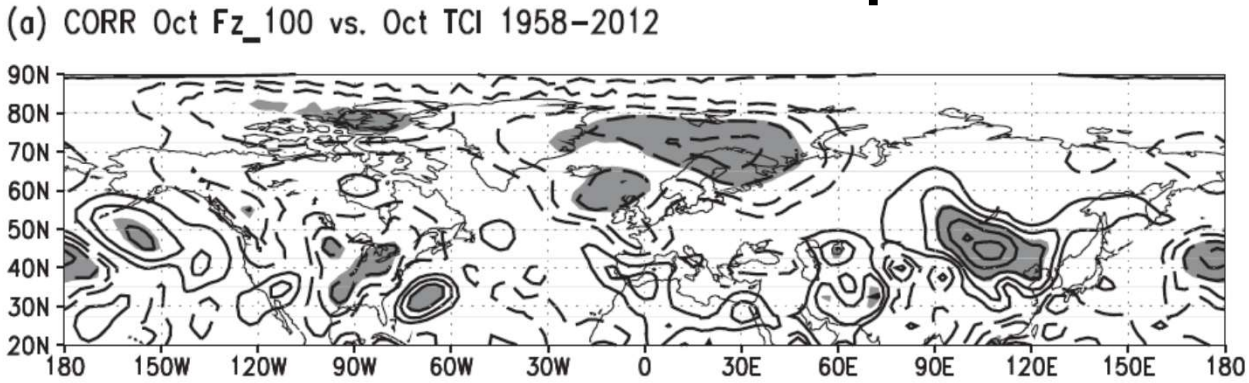

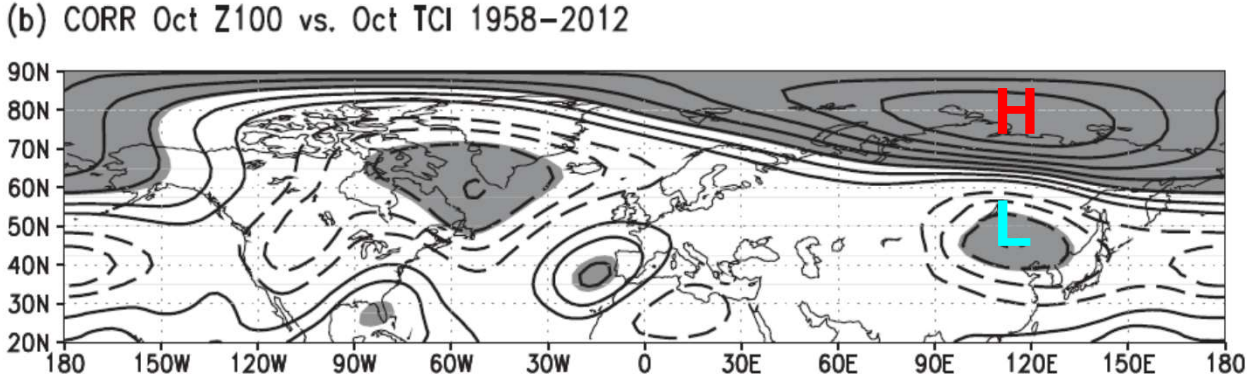

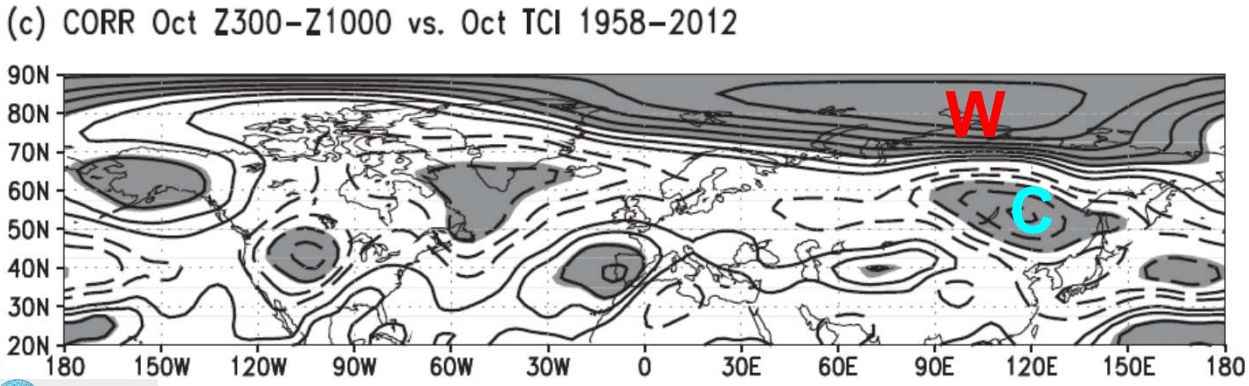

Correlations between the October upward 100-hPa EP flux (a), Z100 (b), 300-1000-hPa layer thickness (c) and the October TCI for 1958 - 2012.

Contour interval is 0.1, negative values are dashed, the 0 value is omitted.

The area where the correlations are significant at the 5% level in a two-tailed test is shaded

B&W figures from Kryjov (2015)

APCC
APEC CLIMATE CENTER

Associated Synoptic Processes and Other Possible Predictors

Composites of October SLP (mb)
for winters of the DJF AOI above the upper quintile, below the lower quintile and their difference.

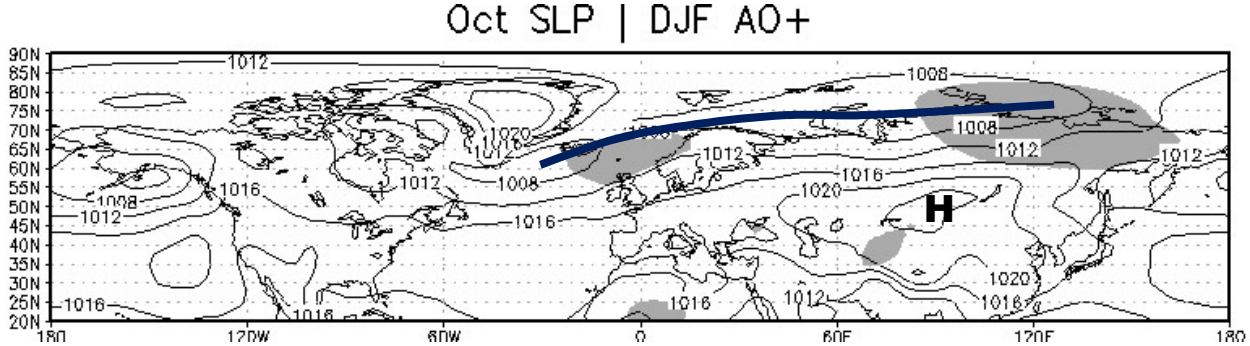

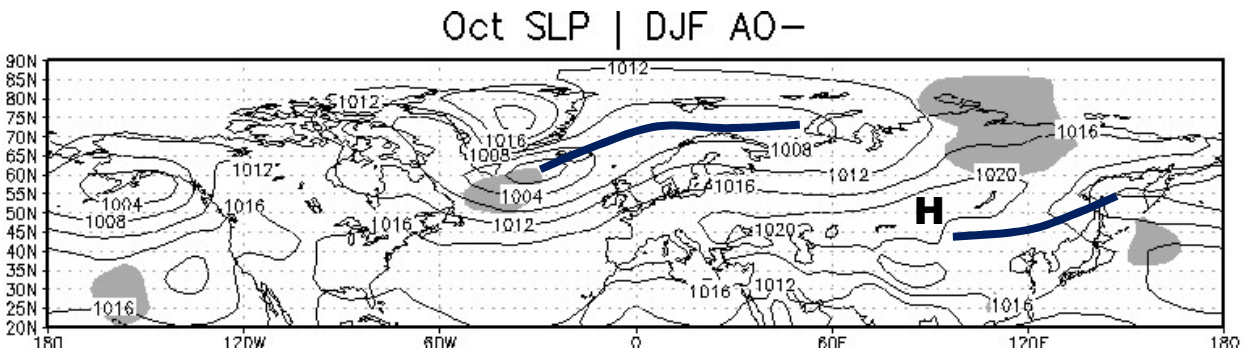

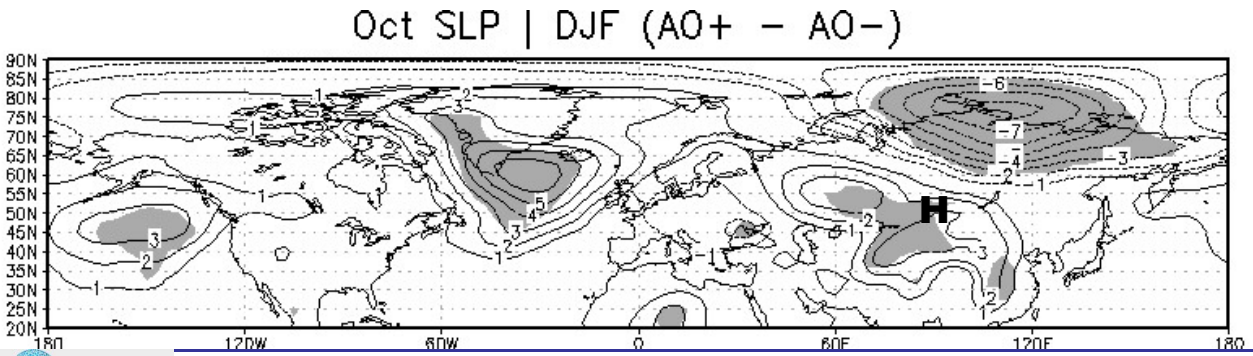

The area where the SLP anomalies and the differences are significant at the 2.5% level in a one-tailed test is shaded.

The letter “H” denotes the October climatological centre of the Siberian High.

Blue bold lines show the axes of the troughs

Composites of October Z500 (m)
for winters of the DJF AOI above the upper quintile, below the lower quintile and their difference.

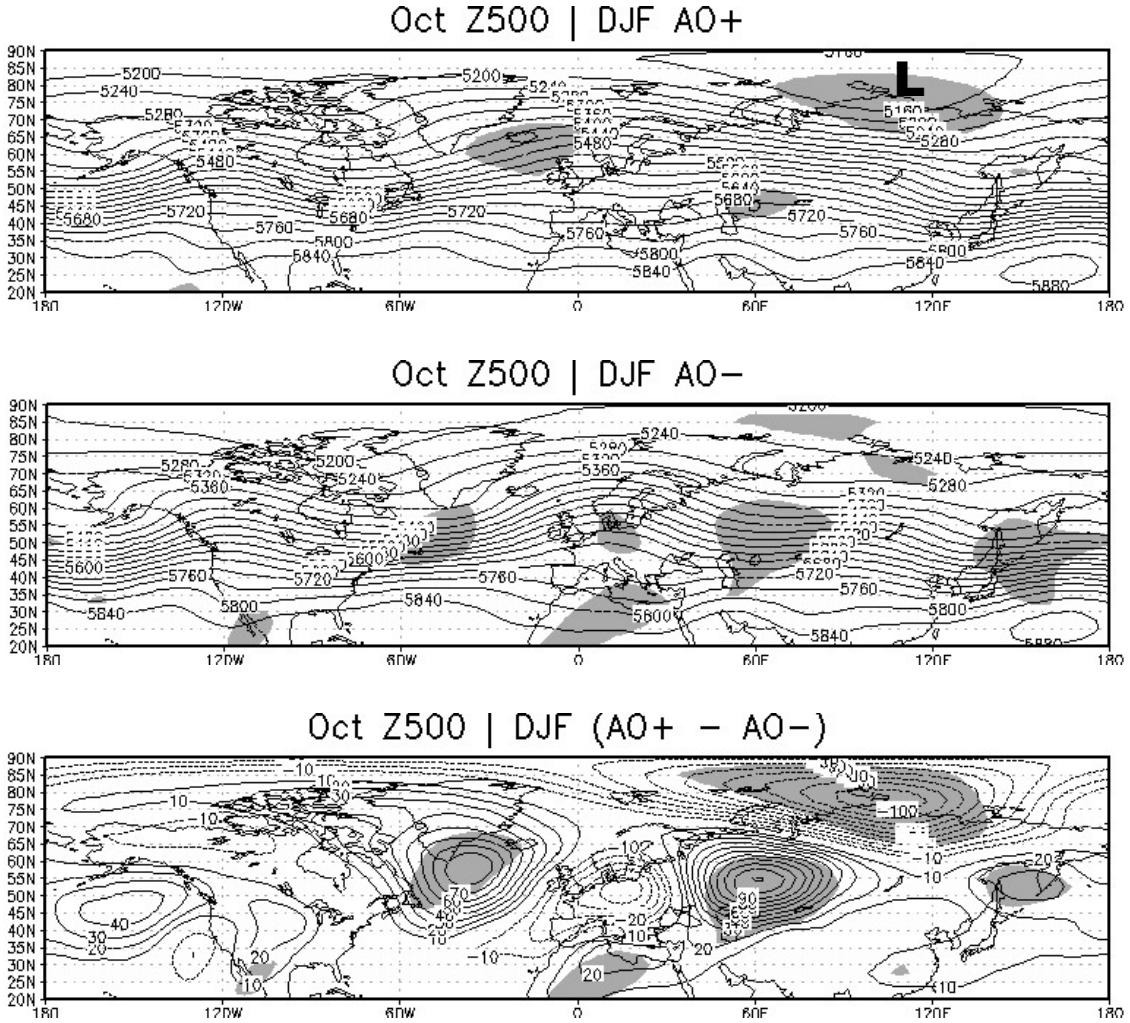

The area where the Z500 anomalies and the differences are significant at the 2.5% level in a one-tailed test is shaded.

The letter “H” denotes the October climatological centre of the Siberian High.

Blue bold lines show the axes of the troughs

Composites of October U300 (m/s)

for winters of the DJF AOI above the upper quintile, below the lower quintile and their difference.

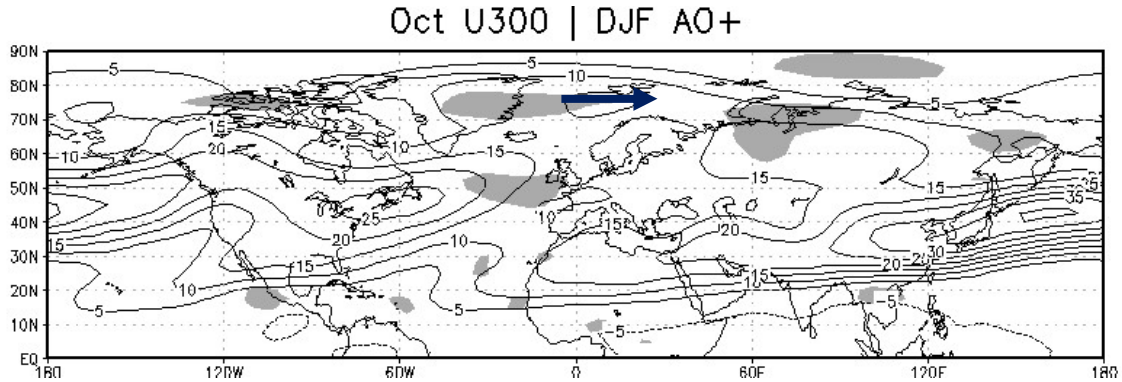

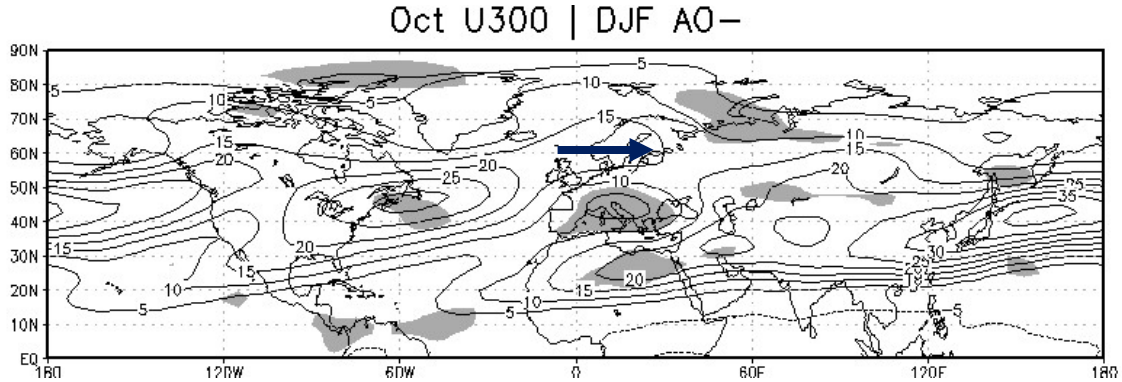

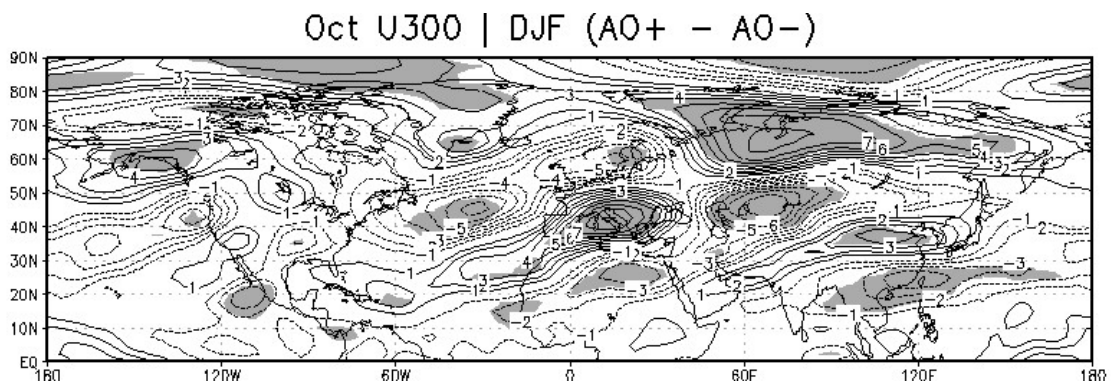

Z500 vs. variable predictors **R_mean**

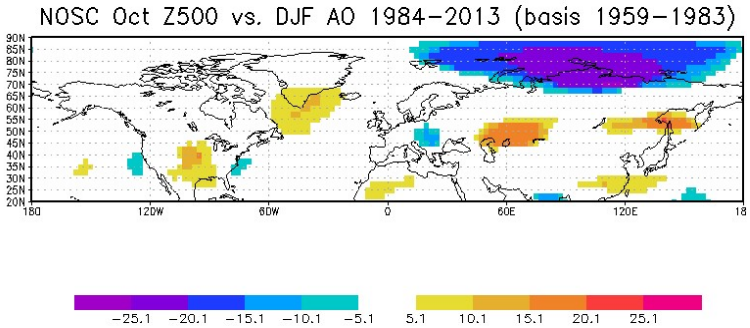

The number of years (out of 30) with correlations underlying regression |R|>0.4

Original correlation maps (30 maps) estimated 30 times based on sliding 25-year training periods

0.91

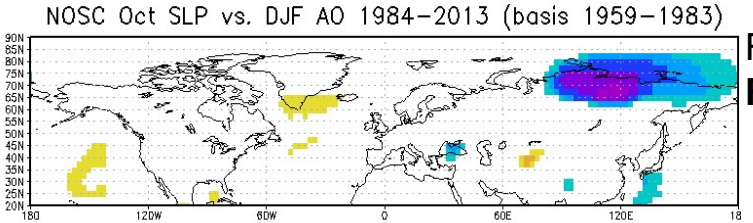

Regr. **R_mean / TCC**

0.63 / 0.40

0.83

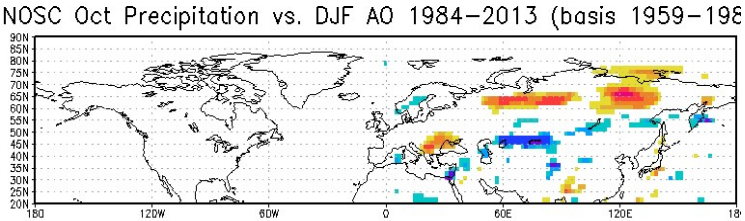

0.91 / 0.26

0.76

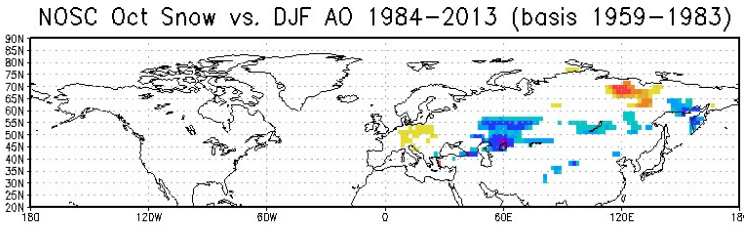

0.79 / 0.40

0.56

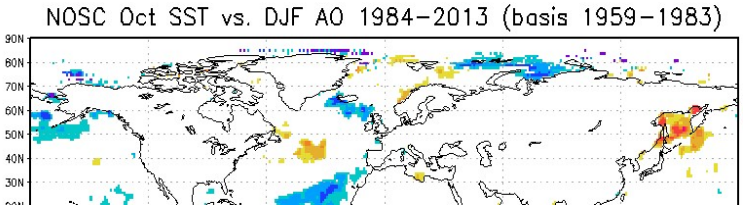

0.71 / 0.31

0.41

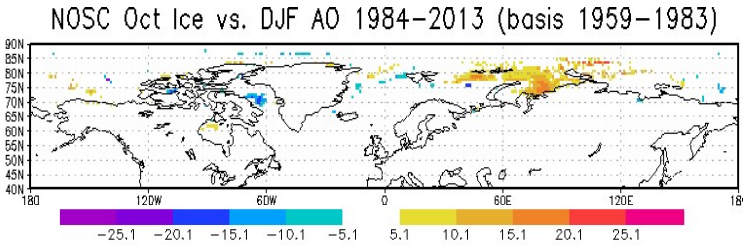

0.79 / 0.32

Conclusions

October Z500 successful predictor patterns tend to resemble a pattern of the Taymyr Circulation Anomaly.

A mechanism linking the DJF AO phase with October circulation is anomalous October heat advection of different signs to the Arctic and to the East Asia.

October synoptic processes preceding the DJF positive AO phase are the northward shift of the PJS, enhancement of Z500 steering flow over the northernmost Eurasia, propagation of Atlantic cyclones up to Taymyr Peninsula and the Laptev sea. Vice versa for DJF negative AO phase.

Assessments based on the series of 30 independent predictions of the wintertime AO reveal correlation between the predicted and observed DJF AOI exceeding 0.6 and MSSS exceeding 0.35.

The carried out analysis yields that seasonal prediction may be based on a certain succession of rapidly varying atmospheric processes starting from certain initial conditions, not only on the slowly varying boundary conditions.

Thank you